

## ASSESSMENT OF MICROSTRUCTURE CHANGES OF STEEL IN STEAM PIPING BY CONVENTIONAL ULTRASONIC TESTING PROBES

<sup>1,2</sup>Tomáš ZAVADIL, <sup>2</sup>Petr ŽBÁNEK, <sup>3</sup>Marie MOŘKOVSKÁ

<sup>1</sup>*Czech Technical University in Prague, Faculty of Nuclear Sciences and Physical Engineering, Prague, Czech Republic, EU, [zavadilt@atg.cz](mailto:zavadilt@atg.cz)*

<sup>2</sup>*ATG - Advanced Technology Group s.r.o., Prague, Czech Republic, EU, [zbanek@atg.cz](mailto:zbanek@atg.cz)*

<sup>3</sup>*VSB - Technical University of Ostrava, Ostrava, Czech Republic, EU, [mar.morkovska@gmail.com](mailto:mar.morkovska@gmail.com)*

<https://doi.org/10.37904/metal.2019.872>

### Abstract

Creep is one of the main phenomena responsible for degradation of material on in-service equipment operated at high temperatures and pressures e.g. steam pipings and superheaters. Process is accompanied by microstructure changes as well as plastic deformation of the equipment that is difficult to measure via conventional NDT. Ultrasonic waves velocity is able to react on changes created due to microstructure changes and due to change of stress-strain conditions. Measurements performed as a part of this article monitors deformation on a cross-section of a steam piping from heat-resistant steel via area scan of ultrasonic waves velocity ratio. Experiments also confirmed that the trend of the velocity ratio along the part's circumference corresponds to the cross-section measurements and is in correlation with hardness development.

**Keywords:** Creep, ultrasonic testing, microstructure, piping

### 1. INTRODUCTION

Creep degradation process is one of the main phenomena responsible for the failure of pressure equipment operated at high temperatures and pressures and is associated with the synergistic effect of microstructural changes and strain accumulation. Since the real life expectancy of operated equipment is based on the ability of the material to retain its high-temperature creep strength for a period of at least twice the projected design life of such equipment, methods that shall be able to assess the material condition based on physical changes occurring during operation are necessary to be developed and used [1]. Various special non-destructive testing applications have been developed to detect creep such as thermography, ultrasonic attenuation and velocity measurements, acoustic harmonic measurements and even eddy currents [2-3]. Other means of evaluation usually require sample extraction, which may not be preferable due to necessity for replacement of extracted equipment component. In this article the author is proposing a non-destructive UT technique of measurement of longitudinal to transversal waves velocity ratio (further as the "L/T ratio"). This technique is expected to be used to detect plastic strain though the whole pipe wall thickness induced by creep. The technique was tested on extracted membrane wall collapsed due to creep by the author in his article [4]. This article only dealt with evaporator pipings of maximal wall thickness of 6 mm, where dramatic changes of material properties throughout the wall thickness weren't assumed. Steam pipings are one of the 3 main pipings subject to creep (beside membrane walls and superheaters) with wall thickness from 30 to 50 mm, which means conditions on the inner and outer surface may differ. That may impact ability to measure L/T ratio changes significantly. This article deals with measurement of the L/T ratio on thick wall steam pipings and demonstrates, that changes in strain conditions caused due to creep are detectable.

### 2. PRINCIPLE OF MEASUREMENT

According to Schneder and Goebbels [5] ultrasonic waves velocities for generally anisotropic material are function of density, strain in the given axis, Lamé's constants, and Murnaghan's constants. Assuming the

tested volume of the material has isotropic behavior, equations for longitudinal ( $c_L$ ) and transversal ( $c_T$ ) ultrasonic waves' velocity may be then determined more simply as the following:

$$c_L = \sqrt{\frac{E}{\rho} \frac{1-\nu}{(1+\nu)(1-2\nu)}} \text{ and } c_T = \sqrt{\frac{G}{\rho}} = \sqrt{\frac{E}{\rho} \frac{1}{2(1+\nu)}} \quad (1)$$

where  $E$  and  $G$  are commonly referred as Young and Shear modulus,  $\rho$  is density and  $\nu$  is the Poisson's ratio. In anisotropic scenario the velocities are also affected by anisotropy in elastic properties and inhomogeneous localization of plastic strain, such as slip bands, creation of point defects and yield vertex which is responsible for degradation of elastic modulus, as described by [6-8].

Velocity changes due to changes in elastic properties are generally within units of a percentage [9]. In order to determine each of the velocities with sufficiently high precision, one needs to measure precisely the path which the wave is propagating as well as time of flight (TOF).

Putting velocities into a ratio allows transforming the problem to a single-variable equation (only variable is the Poisson's ratio) with monotone-increasing features:

$$\frac{c_L}{c_T} = \sqrt{\frac{E}{\rho} \frac{1-\nu}{(1+\nu)(1-2\nu)}} \sqrt{\frac{\rho}{G}} = \sqrt{\frac{2(1-\nu)}{1-2\nu}} = f(\nu) \quad (2)$$

This can help determining current stress-strain conditions as observed by Kumar et al. [10]. Since Young ( $E$ ) and Shear ( $G$ ) modulus tend to vary in the same direction in metal, the Poisson's ratio is dependent on how much each of moduli is affected. The higher the Poisson's ratio the less volume change during deformation.

The evaluation is on ordinal basis. Reference value is compared to the recorded measurements and all differences above defined limit are evaluated as potentially critical. In author's previous article [11], an approximate standard reference range of the L/T ratio for P265GH steel in as-delivered condition was:

$$\left\langle \frac{c_L}{c_T} \right\rangle_{P265|REF} = 1.817 \pm 3 \cdot 0.004 = 1.817 \pm 0.012 \quad (3)$$

where  $\left\langle \frac{c_L}{c_T} \right\rangle_{P265|REF}$  is the L/T ratio reference (benchmark) value range for non-affected (in as-delivered condition) P265GH steel. The value range was calculated by comparing L/T ratio values of similar steels subjected to various heat treatments with temperatures below  $A_{c3}$  (where residual stress and strain effects associated with phase transform do not need to be considered). This benchmark value is accurate only for P265GH steel in as-delivered condition, but based on it will be very similar to all carbon steels including other heat-resistant carbon steels. Changes in L/T ratio caused by variation of chemical properties tend to vary only in the extent of about 1.79 to 1.84 as observed in the same article [12].

### 3. EXPERIMENTAL SETUP

The experiment was performed on a part of steam piping elbow from 15128.9 steel with nominal diameter  $d = 324 \text{ mm}$  (inner/outer radius are labelled  $r/R$ ), nominal wall thickness  $t = 48 \text{ mm}$  and length of  $l = 10 \text{ mm}$  (see **Figure 1(left)**) provided by UJP PRAHA a.s. The part was extracted from the system due to creep-induced cracking on the outer surface. Presence of cracks on the surface was caused by combined effect of creep and bending. Extracted part of piping was divided into samples labeled as seen on the **Figure 1(right)**. Samples EPC21 A-C and EPC21 B-C were subject to tensile tests. Tensile tests were performed prior measurement of L/T ratio as a part of another research, i.e. these two samples were not available for evaluation.

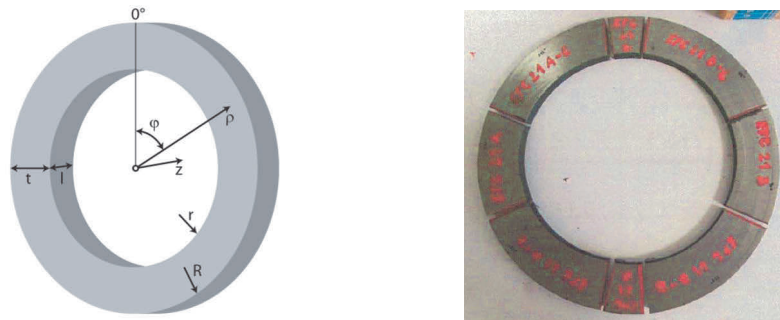


**Figure 1 (left)** drawing demonstrating dimensions of part to be tested. Cylindrical coordinate system  $(\varphi, \rho, z)$  was used to record data **(right)** image of part to be tested divided to individual samples

**Table 1** Samples designation in **Figure 1**, abbreviated designation and  $\varphi$  intervals from the original part covered by these samples

Sample	Abbr.	$\varphi$
EPC21 C	C	$(-5^\circ; 5^\circ)$
EPC21 B-C	B-C	$(5^\circ; 60^\circ)$
EPC21 B	B	$(60^\circ; 105^\circ)$
EPC21 B-D	B-D	$(105^\circ; 165^\circ)$
EPC21 D	D	$(165^\circ; 180^\circ)$
EPC21 A-D	A-D	$(180^\circ; 240^\circ)$
EPC21 A	A	$(240^\circ; 285^\circ)$
EPC21 A	A-C	$(285^\circ; 355^\circ)$

Calibrated UT instrument Sonatest VEO+ with straight beam probes Sonatest FCR2550 with nominal frequency 5 MHz (for longitudinal waves) and Olympus V156-RM with nominal frequency 5 MHz (for transversal waves) were used for measurement of ultrasonic wave velocities.

Due to small length  $l$  the material properties in the  $z$  axis direction may be considered as homogeneous and the L/T ratio may be assumed to be constant throughout the whole length  $l$ . On the other hand for measurement from the outer surface throughout the full wall thickness  $t$  homogeneous properties cannot be assumed and the L/T ratio may therefore vary throughout the thickness. Change of L/T ratio with changing angle  $\varphi$  is given by different strain conditions on elongated and compressed side of the piping.

For these reasons the experiment involved 3 types of measurements:

**A.** net of points measurement of L/T ratio along the  $\varphi$  and  $\rho$  in the direction of  $z$  axis  $\rightarrow c_L/c_T(\varphi, \rho)$ ; **B.** 2-D scanning of L/T ratio along the  $x, y$  Cartesian coordinates with 3mm step in the direction of  $z$  axis; **C.** Line of points measurement along the angle  $\varphi$  in the direction of  $\rho \rightarrow c_L/c_T(\varphi)$

**A) Net of points measurement of L/T ratio along the angle and radius** - Measurement was performed on manually created net of points with angle steps of  $5^\circ$  around the sample surface and with  $\rho$  steps of  $t/5$  starting from the  $\rho = r$  (inner surface) towards  $\rho = R$  (outer surface). Probes were placed on the spots manually, data for both wave types were recorded independently and weren't processed by UT studio software. **B) 2-D scanning of L/T ratio along Cartesian coordinates** - Probes were independently attached on two-axis encoder Phoenix Tracer with 3 mm step recording. Movement of probes was recorded and records analyzed in UT Studio+ software from Sonatest Ltd.  $(x; y)_i = (0; 0)_i$  for each sample  $i$  was set such that the movement of probes on the sample surface always resulted in positive  $x_i$  and  $y_i$  (requirement of the Phoenix Tracer

encoding system). As a result, it was not possible to create unified Cartesian coordinate system for all the samples. **C) Line of points measurement of microstructure changes from piping surface** - Measurement was performed at the same angles as the measurement (A) but from the outer surface in direction to the center of coordinate system. Probes were placed on the spots manually, data were recorded independently and weren't processed by UT studio.

## 4. RESULTS

In order to ensure easy readability of the recorded data, all samples were put together to one figure for each kind of measurement. Data for measurements (A) and (C) were merged together to demonstrate correlation between the data throughout the thickness and the data measured from the outer surface (**Figure 2**). Data recorded by two-axis encoder are displayed in separate last figure below.

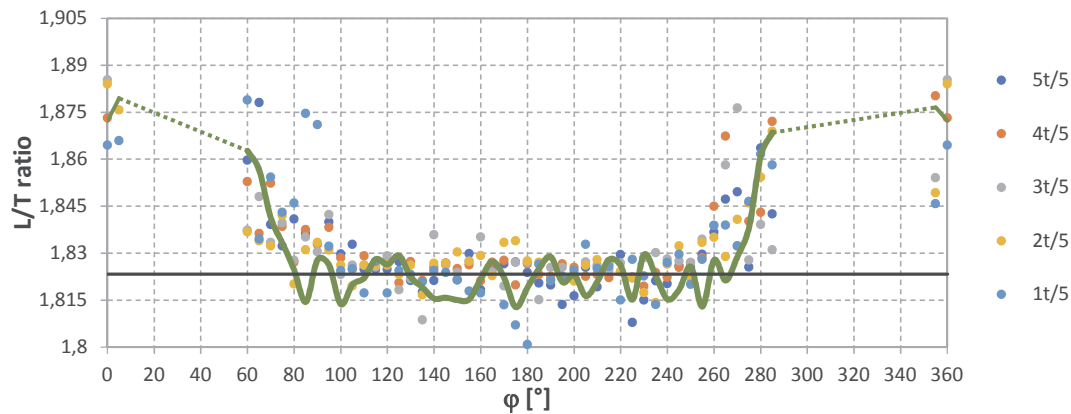


**Figure 2** L/T ratio values measured by measurement (A) at angles  $\{0^\circ; 5^\circ; \dots; 355^\circ; 360^\circ\} \in \varphi$  and radii,  $\{\frac{t}{5}; \frac{2t}{5}; \dots; \frac{5t}{5}\} \in \rho$ . Integral L/T ratio value  $\langle L/T \text{ ratio} \rangle_{\text{int}}$  measured by (C) measurement are included to the chart.  $\langle L/T \text{ ratio} \rangle_{\text{ref}}$  is a reference mean value calculated from measurement (A) data for  $\varphi \in (105^\circ; 240^\circ)$

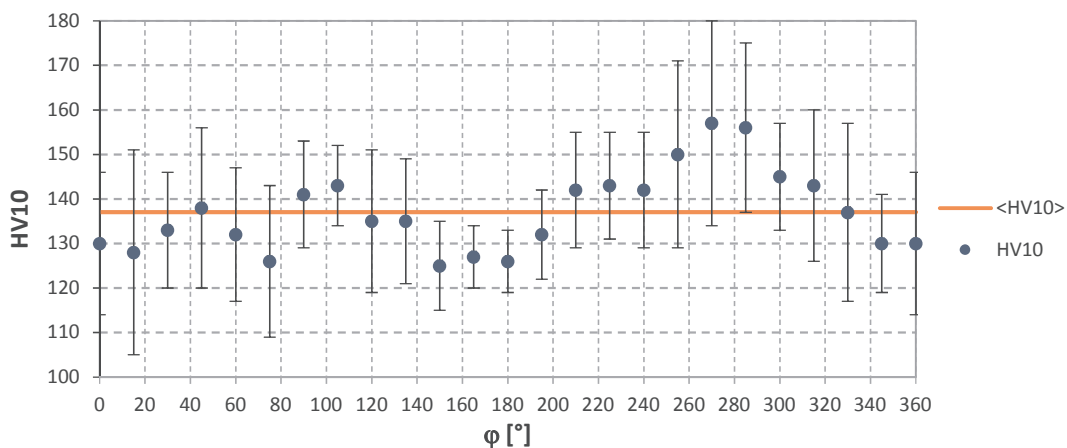


**Figure 3** Vickers hardness HV10 measured at angles  $\{0^\circ; 15^\circ; \dots; 345^\circ; 360^\circ\} \in \varphi$  and mean value  $\langle HV10 \rangle$

Data measured by measurement (A) shown trend of L/T values oscillating around mean reference value  $\langle L/T \text{ ratio} \rangle_{\text{ref}} = 1.8233$  in the range of  $\varphi \in (105^\circ; 240^\circ)$  corresponding to unaffected material acc. to Eq. (3). Values sharply increased outside of this interval to about 1.86  $\varphi \rightarrow 60^\circ_+$  and 1.88 for  $\varphi \rightarrow 285^\circ_-$ . Due to missing samples A-C and B-C their trend of L/T ratio is not known. Hardness testing measured along the outer circumference (performed prior tensile test), shown maximum values at  $\varphi \in (255^\circ; 285^\circ)$  (see **Figure 3**).

Data collected by two-axis encoder were analyzed by UT studio. Raster and color scale were performed in MS Excel due to lacking such functionality in UT Studio software. The orientation of the raster is given by relative Cartesian coordinate system for each of the samples.

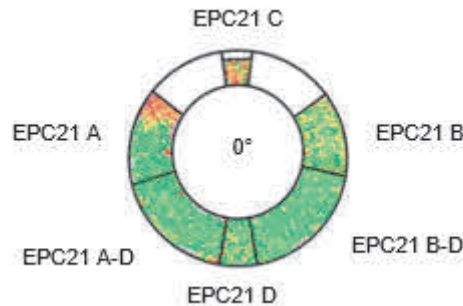


**Figure 4** Measurement of L/T ratio by two-axis encoder. The color scale was set to green for L/T ratio = 1.80, yellow to 1.85 and red to 1.90. Pink spots have missing one of the velocities (either for longitudinal or transversal waves). White spots indicate no values measured for neither of wave types.

Data observed on **Figure 4** intend to demonstrate in more detail how L/T ratio may be developing with changing  $\varphi$  and  $\rho$ . It is visible, that L/T ratio values tend to increase on both sides of the interval  $\varphi \in \langle 60^\circ; 285^\circ \rangle$ . L/T ratio values for  $\varphi \rightarrow 60^\circ_+$  are rather slightly elevated with nominal values around 1.85, whereas values close to  $\varphi \rightarrow 285^\circ_-$  shown more steep increase of L/T ratio, reaching on some places up to 1.95. Change of L/T ratio with increasing  $\rho$  was observed locally in intervals  $\varphi \in \langle 60^\circ; 105^\circ \rangle$  and  $\varphi \in \langle 275^\circ; 285^\circ \rangle$ .

## 5. DISCUSSION

Measurement of L/T ratio from the piping's cross-section (A) and along the outer surface (C) both shown detectable increase of L/T ratio values in areas with increased values of Vickers hardness (HV10) measured from the surface. Previous observation of the author in article [4] shown that average through-thickness hardness strongly correlated with L/T ratio values. As shown on **Figure 2**, L/T ratio steep increase of L/T ratio values for  $\varphi \rightarrow 285^\circ_+$  (maximum 1.877) is in accordance with this claim. Values on the other side of the measured interval for  $\varphi \rightarrow 60^\circ_-$  (maximum 1.862) does not have so much steep increase and it is less pronounced on the hardness chart. That might be a result of partial plastization of this area, where surface hardness is not significantly affected yet, but subsurface conditions are already exceeding standard levels.

Both measurements (A) and (C) shown a relatively stable L/T ratio value in the interval of  $\varphi \in \langle 100^\circ; 240^\circ \rangle$  with mean value  $\langle \text{L/T ratio} \rangle_{\text{ref}}$  equal to 1.8233, which is close to the calculated upper bound of the reference L/T ratio interval for P265GH steel in Eq. (3) [12]. This value was observed on compressed side of the part, it is likely that  $\langle \text{L/T ratio} \rangle_{\text{ref}}$  for as-delivered conditions would have higher L/T ratio (e.g. close to 1.84).

Measurements (A) and (C) shown strong mutual correlation. It was assumed that total L/T ratio value measured from the surface of a sample should be (approx.) equal to average value in its cross-section, i.e.:

$$\frac{c_L}{c_T}(\varphi)_{\rho=R} \sim \frac{1}{R-r} \int_r^R \frac{c_L}{c_T}(\rho)_\varphi d\rho \quad (4)$$

Measurement (B) was designed to get detailed information about the through-thickness L/T ratio. Detailed comparison of **Figure 2** and **Figure 4** confirms that the assumption in Eq. (4) is principally correct. It means measurement of L/T ratio from the surface provides integral value of the tested volume and reacts to changes equally no matter the depth under the surface. Due to the fact changes of L/T ratio along  $\rho$  were observed only on limited intervals of  $\varphi$  a threshold of detectability was not able to be retrieved reliably (it was not possible to define reliably how big part of the sample needs to be affected to show measurable change). This topic shall be

assessed in future experiments. Measurements however confirmed that even on piping samples with potentially heterogeneous properties throughout the wall thickness L/T ratio may provide important information about change of material characteristics for effective detection of creep deformation.

## 6. CONCLUSION

The article aimed to solve a partial research topic dealing with ability of UT technique of longitudinal to transversal ultrasonic waves velocity ratio introduced by the author to detect creep deformation on thick wall samples as e.g. steam pipings. The experiment was performed on piping extracted due to presence of creep cracking. The article confirms that the ultrasonic waves' velocity ratio measurement is able to find changes of microstructure and stress-strain conditions of the piping wall when measured from the outer surface even where the material cannot be considered as homogeneous throughout the thickness due to its significant thickness. In order to define threshold of detectability, further experiments need to be performed. This is one of the topics of current research of authors.

## ACKNOWLEDGEMENTS

*This article is a part of ongoing postgraduate studies of the main author. Valuable discussions with Mr. Jaroslav Pitter, Ph.D. (materials and corrosion specialist, thesis advisor) are gratefully acknowledged.*

## REFERENCES

- [1] SKLENIČKA, V., KUCHAROVÁ, K., SVOBODA, M., KLOC, L., BURŠÍK, J. and KROUPA, A. Long-term creep behavior of 9-12%Cr power plant steels. *Materials characterization*. 2003. vol. 51, pp 35-48.
- [2] BABY, S., KOWMUDI, N., OMPRAKASH, C.M., SATAYABARAYANA, D.V.V., BALASUBRAMANIAM, K. and KUMAR, V. Creep damage assessment in titanium alloy using nonlinear ultrasonic technique. *Scripta Materialia*. 2008, vol. 59, pp 818-821.
- [3] SPOSITO, G., WARD, C., CAWLEY, P., NAGY, P.B. and SCRUBY, C. A review of non-destructive techniques for the detection of creep damage in power plant steels. *NDT&E International*. 2010. vol. 43, pp 555-567.
- [4] Zavadil, T. Detection of Creep Degradation on Collapsed Membrane Wall From P265GH Pressure Purpose Steel by Ultrasonic Testing. *In ASME 2018 Pressure Vessels and Piping Conference*. Prague: Czech Tech. Univ., 2018, pp. 632-637.
- [5] SCHNEDER, R. and GOEBBELS, K. Zertörungdfreie Bestimmung von Eigenspannungen mit linear polarisierten Ultraschallwellen. *VDI Berichte*. 1982. No. 439.
- [6] KOBAYASHI, M. Acoustoelastic Theory for Plastically Deformed Solids. *JSME International Journal*. 1990. vol. 33, no. 3, pp 310-318.
- [7] KOBAYASHI, M. Ultrasonic Nondestructive Evaluation of Microstructural Changes of Solid Materials Under Plastic Deformation - Part I. Theory. *International Journal of Plasticity*. 1998. vol. 14, no. 6, pp 511-522.
- [8] KOBAYASHI, M. Analysis of deformation localization based on proposed theory of ultrasonic wave velocity propagating in plastically deformed solids. *International Journal of Plasticity*. 2010. vol. 26, pp 107-125.
- [9] OBRAZ, V. *Zkoušení materiálu ultrazvukem*. 1st ed. Prague: SNTL, 1989, p. 251.
- [10] KUMAR, A., JAYAKUMAR, T., RAJ, B. and RAY, KK. Correlation between ultrasonic shear wave velocity and Poisson's ratio for isotropic solid materials. *Acta Materialia*. 2003. vol. 51, pp 2417-2426.
- [11] Zavadil, T. Selection of Reference Value of Longitudinal to Transversal Ultrasonic Waves Velocity Ratio on Pressure Purpose Steels for Detection of Creep. *Acta Polytechnica CTU Proceedings*. 2018. Vol. 19, pp 46-52.